OPEN ACCESS
CellPress

Cell Reports
Report

Hypothalamic Contribution to Pituitary Functions Is Recapitulated *In Vitro* Using 3D-Cultured Human iPS Cells

Takatoshi Kasai,[1] Hidetaka Suga,[1,6,*] Mayu Sakakibara,[1] Chikafumi Ozone,[1] Ryusaku Matsumoto,[2] Mayuko Kano,[1] Kazuki Mitsumoto,[1] Koichiro Ogawa,[1] Yu Kodani,[3] Hiroshi Nagasaki,[3] Naoko Inoshita,[4] Mariko Sugiyama,[1] Takeshi Onoue,[1] Taku Tsunekawa,[1] Yoshihiro Ito,[1] Hiroshi Takagi,[1] Daisuke Hagiwara,[1] Shintaro Iwama,[1] Motomitsu Goto,[1] Ryoichi Banno,[1] Jun Takahashi,[5] and Hiroshi Arima[1]

[1]Department of Endocrinology and Diabetes, Nagoya University Graduate School of Medicine, Nagoya 466-8550, Japan
[2]Division of Diabetes and Endocrinology, Department of Internal Medicine, Kobe University Graduate School of Medicine, Kobe 650-0017, Japan
[3]Department of Physiology, Fujita Health University, Toyoake 470-1192, Japan
[4]Department of Diagnostic Pathology, Toranomon Hospital, Tokyo 105-8470, Japan
[5]Department of Clinical Application, Center for iPS Cell Research and Application, Kyoto University, Kyoto 606-8507, Japan
[6]Lead Contact
*Correspondence: sugahide@med.nagoya-u.ac.jp
https://doi.org/10.1016/j.celrep.2019.12.009

SUMMARY

The pituitary is a major hormone center that secretes systemic hormones responding to hypothalamus-derived-releasing hormones. Previously, we reported the independent pituitary induction and hypothalamic differentiation of human embryonic stem cells (ESCs). Here, a functional hypothalamic-pituitary unit is generated using human induced pluripotent stem (iPS) cells *in vitro*. The adrenocorticotropic hormone (ACTH) secretion capacity of the induced pituitary reached a comparable level to that of adult mouse pituitary because of the simultaneous maturation with hypothalamic neurons within the same aggregates. Corticotropin-releasing hormone (CRH) from the hypothalamic area regulates ACTH cells similarly to our hypothalamic-pituitary axis. Our induced hypothalamic-pituitary units respond to environmental hypoglycemic condition *in vitro*, which mimics a life-threatening situation *in vivo*, through the CRH-ACTH pathway, and succeed in increasing ACTH secretion. Thus, we generated powerful hybrid organoids by recapitulating hypothalamic-pituitary development, showing autonomous maturation on the basis of interactions between developing tissues.

INTRODUCTION

Pituitary hormones are essential to support a wide variety of physiological functions. Dysfunctions of these hormones cause various systemic symptoms. For example, adrenocorticotropic hormone (ACTH) deficiency causes secondary adrenal insufficiency that can be fatal. Steroid replacement is the standard therapy for ACTH deficiency, but even treated patients are at high risk for acute adrenal insufficiency and death (Burman et al., 2013; Hahner et al., 2015; Sherlock et al., 2010). Such patients are also more likely to develop diabetes, hypertension, and depression, mainly because steroid replenishment tends to be excessive (Stewart et al., 2016). It is difficult to replace the appropriate amount of hormones, largely because the levels of ACTH and downstream cortisol vary greatly depending on the time and surrounding environments (Sherlock et al., 2010; Cooper and Stewart, 2003; Vermes et al., 1995).

Currently, regenerative medicine using pluripotent stem cells is progressing in various fields (Schwartz et al., 2016; Doi et al., 2014; Nakamura and Okano, 2013). If we can generate human anterior pituitary tissue that is adequately responsive to the surrounding environment, such an approach can be applied to regenerative medicine for pituitary disorders and will likely be superior to the current replacement therapy.

Several studies have reported methods to differentiate human pluripotent stem cells into anterior pituitary *in vitro* (Ozone et al., 2016; Dincer et al., 2013; Zimmer et al., 2016). We have also succeeded in generating a functional anterior pituitary from mouse and human embryonic stem cells (ESCs) (Ozone et al., 2016; Suga et al., 2011). Our method places emphasis on reproducing developmental processes using three-dimensional (3D) culture. Specifically, we used 3D culture called SFEBq (serum-free floating culture of embryoid body-like aggregates with quick reaggregation) (Eiraku et al., 2008), which induces ectodermal tissue with high quality.

RESULTS

Inducing Human iPS Cells to Differentiate into the Anterior Pituitary

As the first step, we verified human induced pluripotent stem (iPS) cell differentiation into the anterior pituitary using the same method applied to human ESCs (Ozone et al., 2016), as shown in Figure 1A. We refer to this differentiation method as the ''original condition'' in this report. The differentiation experiments were performed using a common iPS cell line, 201B7. On day 30, two layers of RX^+ hypothalamic precursor-like tissue in the interior and pan-cytokeratin$^+$ oral ectoderm-like tissue

This is an open access article under the CC BY license (http://creativecommons.org/licenses/by/4.0/).

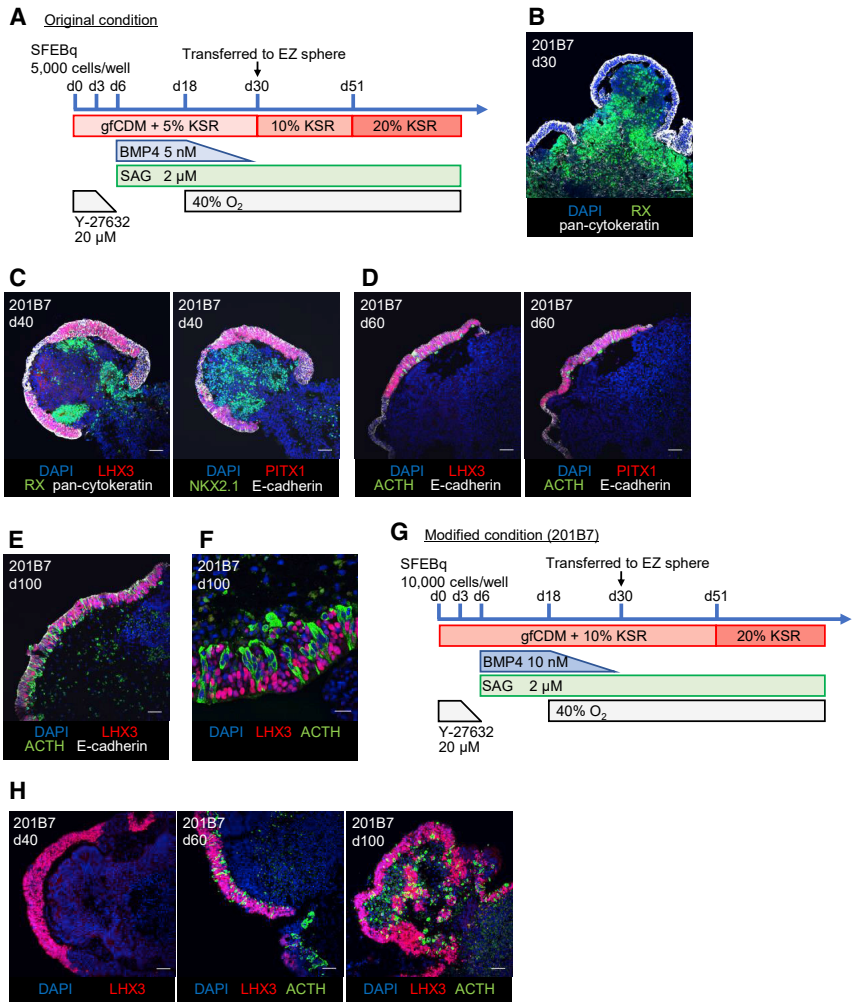

Figure 1. Induction of Human iPS Cells to Differentiate into Anterior Pituitary

(A) Culture conditions to induce human ESCs to differentiate into anterior pituitary (original condition).

(B–F) Induction of the human iPS cell line 201B7 to differentiate into anterior pituitary using the same method used for human ESCs.

(B) Two layers of RX^+ hypothalamic precursor-like tissue in the interior and pan-cytokeratin$^+$ oral ectoderm-like tissue in the periphery.

(C) Oral ectoderm-like tissue expressed pituitary progenitor markers (LHX3, PITX1, and E-cadherin).

(D and E) $ACTH^+$ cells were present in the oral ectoderm-like tissue.

(F) LHX3 expression in $ACTH^+$ cells was attenuated on day 100.

(G) Modified condition for the human iPS cell line 201B7.

(H) Expression of LHX3 and ACTH, as determined by immunostaining, was extensive under the modified conditions.

Scale bars: 50 μm (B–E and H) and 20 μm (F).

were formed at the periphery (Figure 1B). On day 40, expression of the early pituitary marker LHX3 was intensified. $LHX3^+$ oral ectoderm-like tissue also expressed PITX1 and E-cadherin, which are markers of pituitary progenitor cells (Figure 1C). RX^+ and $NKX2.1^+$ ventral hypothalamus-like tissue was present in the interior, adjacent to oral ectoderm-like tissue. $ACTH^+$ cells were observed on day 60 (Figure 1D). With continuous incubation, more $ACTH^+$ cells were observed on day 100 (Figure 1E). LHX3 expression in $ACTH^+$ cells was attenuated on day 100 (Figure 1F). These data indicate that human iPS cell line 201B7 is capable of differentiating into anterior pituitary cells under the same conditions used for human ESCs.

We next attempted to improve the efficiency of differentiation. Because LHX3 has been correlated with subsequent ACTH expression, we optimized the efficiency of LHX3 expression on day 40 by modifying the initial (days 0–30) culture conditions. Specifically, we examined five factors: the initial number of cells per well, the concentration of KSR added to growth factor-free chemically defined medium (gfCDM), bone morphogenetic protein 4 (BMP4) concentration, smoothened agonist (SAG; for activation of the Sonic hedgehog pathway) concentration, and the timing of BMP4 addition (Figure S1A). The aggregates became cystic and morphologically defective when SAG was added later than BMP4. Therefore SAG addition was started at the same time as BMP4 addition. We optimized each factor separately and then combined the individual parameters as the "modified condition." Although no statistically significant difference was observed for each factor (Figures S1B–S1F), LHX3 expression appeared to be higher using 10,000 cells per well, 10% KSR, 10 nM BMP4 during days 6–15, and 2 μM SAG. We determined the "modified condition" as shown in Figure 1G by combining the factors. As shown in Figure 1H, $LHX3^+$ cells and $ACTH^+$ cells were abundant, although there were no significant differences during days 40–60. Finally, on day 100, the proportion of $ACTH^+$ cells was significantly elevated under the modified condition (Figures S1G–S1K, S2A, and S2B). qPCR analyses did not detect any differences between the original and modified conditions (Figures S1L–S1P), but the final ACTH concentration in culture supernatants on day 100 was significantly higher under the modified condition (Figures S1Q and S1R).

Next, we performed similar experiments using other iPS cell lines, 409B2 and 454E2. In 409B2 cells, LHX3 expression was confirmed on day 40, and $ACTH^+$ cells were detected on days 60 and 100 under the original condition (Figure S3A). We next decided the modified condition in the same manner as 201B7 (Figure S3B). However, neither $LHX3^+$ nor $ACTH^+$ cells showed any differences under the modified condition compared with the original condition (Figures S3C–S3H). In 454E2 cells, expression of LHX3 and ACTH was also confirmed under the original condition (Figure S3I). We tried to modify the differentiation condition (Figure S3J), but there were no differences (Figures S3K–S3P).

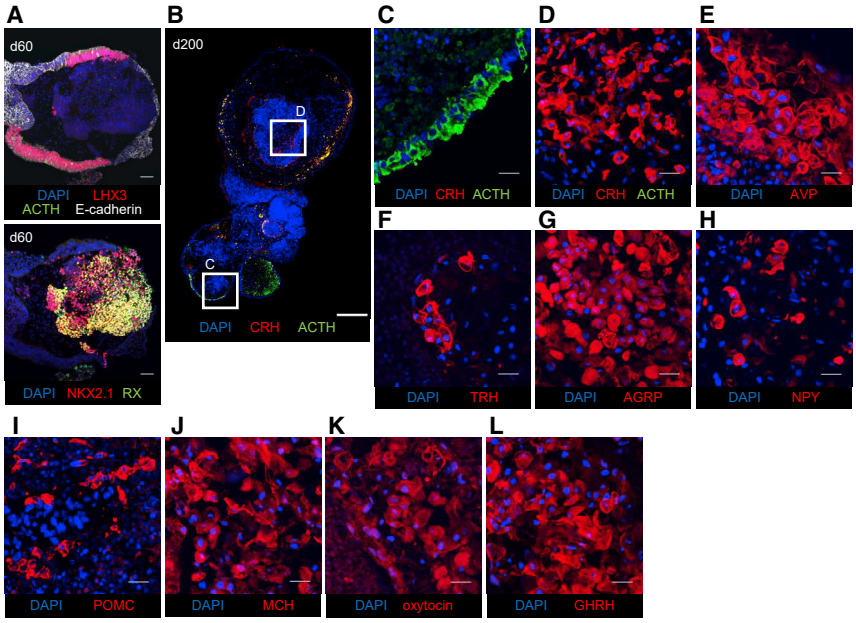

Figure 2. Both Anterior Pituitary and Hypothalamic Neurons Were Developed Simultaneously

(A) Hypothalamic precursor tissue (RX$^+$, NKX2.1$^+$) was adjacent to anterior pituitary tissue (ACTH$^+$, LHX3$^+$, E-cadherin$^+$).

(B–D) ACTH$^+$ cells and CRH$^+$ cells coexisted in the same aggregates. The whole image of the aggregate is (B). Anterior pituitary area which is pheriphery of aggregate is (C), and hypothalamic area which is inner layer of aggregate is (D).

(E–L) Hypothalamic hormone-positive cells. AVP (E), TRH (F), AGRP (G), NPY (H), POMC (I), MCH (J), oxytocin (K), and GHRH (L).

Scale bars: 500 μm (B), 50 μm (A), and 20 μm (C–L).

These data show that all three types of human iPS cells are capable of differentiating into anterior pituitary cells under the same conditions as human ESCs, although the low efficiency and large variations remain problems to be resolved in the future.

Simultaneous Development of Both Anterior Pituitary and Hypothalamic Neurons

Because tissue interactions with the hypothalamus are considered important for the development of the anterior pituitary in embryos (Takuma et al., 1998; Rizzoti and Lovell-Badge, 2005; Zhu et al., 2007; Scully and Rosenfeld, 2002), we next focused on hypothalamic tissue in human iPS cell aggregates. The following experiments were performed using 201B7 human iPS cells under the modified condition shown in Figure 1G. At the early stage of anterior pituitary induction, hypothalamic precursor-like tissue was also induced in the same aggregates. RX$^+$ and NKX2.1$^+$ hypothalamic precursor-like tissue was adjacent to the anterior pituitary tissue on day 60 (Figure 2A). Around the time that ACTH$^+$ cells appeared on day 60, we investigated whether the hypothalamic tissue in the inner layer had matured. We did not detect hypothalamic hormone-positive cells in the hypothalamic area at this time. Therefore, we continued long-term culture. At around day 200, CRH$^+$ cells appeared in the inner layer of aggregates (i.e., the hypothalamic area) (Figures 2B–2D and S4A). Maturation of hypothalamus-like cells also appeared to proceed, as reflected by the presence of cells positive for other hormones (e.g., AVP, NPY, and TRH) in the hypothalamus (Figures 2E–2L). Hereafter, we refer to aggregates that contain co-existing tissues as "hybrid aggregates."

Equivalent Capacity for ACTH Secretion as Adult Mouse Pituitary Cells

ACTH secretion values continued to increase as the culture period was extended at least until day 300 (Figure 3A). Ultrastructurally, the majority of endocrine cells were angular shaped with ovoid nuclei and filled with well-developed Golgi complexes, rough endoplasmic reticulum, and free ribosomes. Cytoplasmic storage secretory granules were numerous. These granules measured 300–1,000 nm, showing characteristic teardrop or heart shapes. The bundle of intermediate filaments, which is one of the specific markers of mature corticotrophs, was not prominent but existed (Figures 3B and 3C). Immunogold labeling revealed ACTH on secretory granules (Figure 3D). Hybrid aggregates were also induced during long-term culture under the original condition (Figures S4B and S4C), suggesting that the ACTH secretion capacity of the aggregates was increased along with hypothalamic maturation.

Next, we evaluated the effect of the hypothalamus on maturation of the anterior pituitary in long-term culture. To this end, we manually separated day 70 aggregates into the anterior pituitary and hypothalamus portions, cultured each portion for 150 days under several conditions, and then measured ACTH values (Figure 3E). Single culture of the isolated anterior pituitary portion resulted in very little ACTH secretion. In contrast, ACTH secretion was partially but significantly recovered when the anterior pituitary and hypothalamus portions were re-combined and cultured adjacent to each other. ACTH secretion was also partially recovered when cultures of the anterior pituitary portion were supplemented with FGF, a hypothalamic factor (Figures 3F, S4D, and S4E). Addition of another hypothalamic factor, BMP4 (Figure 3G), partially recovered ACTH secretion in the same manner. Excessive BMP4 (10 nM) resulted in cystic oral ectodermal tissue (Figure 3H). These results suggested that the presence of the hypothalamus is important in not only the early stage of anterior pituitary differentiation but also the maturation stage.

Next, we determined the level of ACTH secretion from the hybrid aggregates. To compare our aggregates with the *in vivo* pituitary gland, we performed a cell immunoblot assay (CIBA) (Arita et al., 1993) to measure ACTH secretion from single cells. ACTH secretion from 201B7-derived pituitary cells on day 150 was 0.507 ± 0.039 pg/mL per cell versus 0.499 ± 0.040 pg/mL per cell from adult (12-month-old) mouse pituitary (Figure 3I). These data indicated that the hybrid aggregates were

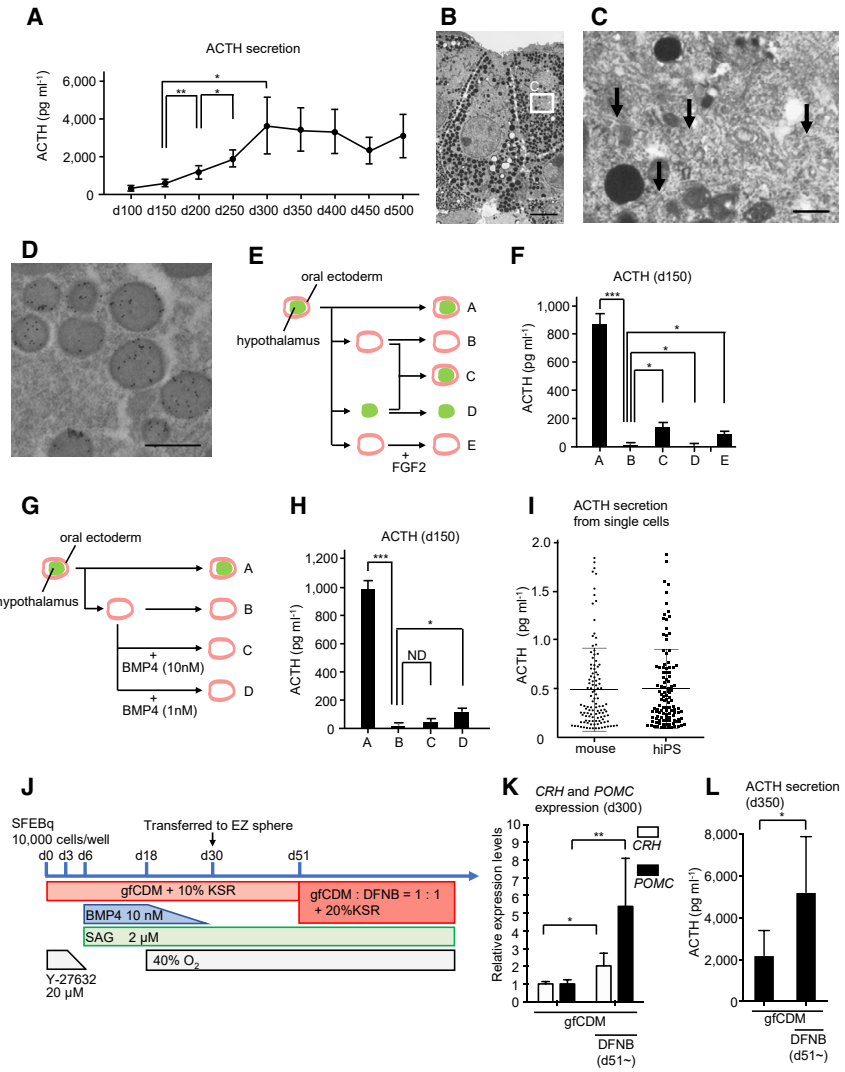

Figure 3. Simultaneous Development of Both Anterior Pituitary and Hypothalamic Neurons, Resulting in an Equivalent Capacity of ACTH Secretion as Adult Pituitary Cells

(A) ACTH value in the culture medium of long-term cultures (n = 17 experiments).

(B–D) Electron micrograph (B and C) and immunoelectron micrograph (D) of human iPS cell-derived corticotrophs on day 500. Arrows in (C) indicate intermediate filament bundles.

(E–H) Culture in which the anterior pituitary and hypothalamic portions were separated.

(E and G) Schematic of the culture process.

(F and H) ACTH level in the culture medium (n = 3 experiments).

(I) ACTH secretion from single cells in aggregates derived from human iPS cells or the anterior pituitary gland from adult mice (n = 3 experiments).

(J) Schema of culture conditions for both pituitary and hypothalamus maturation after day 51.

(K) Expression of CRH and POMC on day 300 (qPCR; n = 5 experiments).

(L) ACTH secretion from aggregates on day 350 (n = 5 experiments).

Scale bars: 5 μm (B) and 0.5 μm (C and D). Values shown on graphs represent means ± SEM. *p < 0.05, **p < 0.01, and ***p < 0.001.

comparable with the *in vivo* pituitary gland, at least with regard to their ACTH secretion capacity. Furthermore, we modified the culture medium for hypothalamic differentiation (Figure 3J) on the basis of our previous study (Ogawa et al., 2018). As a result, increased CRH induction (Figure 3K) appeared to promote ACTH maturation (Figure 3L).

Functional Hypothalamic-Pituitary Axis in Hybrid Organoids

The simultaneous maturation of anterior pituitary and hypothalamic neurons led us to examine whether these two tissues cooperate, because the hypothalamic-pituitary axis is a very important cascade.

First, we evaluated the functionality of ACTH cells in aggregates in which both anterior pituitary and the hypothalamus were induced under the modified condition shown in Figure 1G. Following CRH stimulation, the ACTH concentration in the medium was increase by ~2-fold (Figure 4A). Immunohistochemical analyses revealed that almost all ACTH-positive cells expressed CRH-R1 (Nigawara et al., 2003; Figure 4B), the primary receptor for CRH (Perrin and Vale, 1999). These data demonstrated that ACTH-positive cells responded normally to exogenous CRH stimulation and secreted ACTH. We next investigated negative feedback. When the glucocorticoid dexamethasone was added to the medium, the ACTH level was decreased by ~2-fold halved (Figure 4C), indicating that the aggregates retained negative feedback properties (Figure 4D).

Second, we examined hypothalamic CRH control of pituitary ACTH cells. To evaluate whether the anterior pituitary functioned under the control of the hypothalamus in our induced aggregates, we added the CRH receptor 1 inhibitor antalarmin (Webster et al., 1996) or NBI 27914 (Hoare et al., 2003) to the medium and then measured ACTH. The ACTH level was decreased by ~30% in response to antalarmin treatment (Figure 4E) and by 15% in response to NBI 27914 treatment (Figure 4F), suggesting that $ACTH^+$ cells in the anterior pituitary functioned under the control of CRH-producing cells (Figure 4G). Next, we investigated the effect of CRH neuron stimulation on the downstream ACTH level. In general, ACTH is secreted from the anterior pituitary through hypothalamic neurons such as CRH under hypoglycemic stimulation (Plotsky et al., 1985). Therefore, we applied low glucose exposure as the stimulating signal for CRH neurons and compared ACTH secretion into low-glucose medium (10 mg/dL glucose) and normal-glucose medium (100 mg/dL glucose). The ACTH level increased by about 3-fold in low-glucose medium compared with normal-glucose

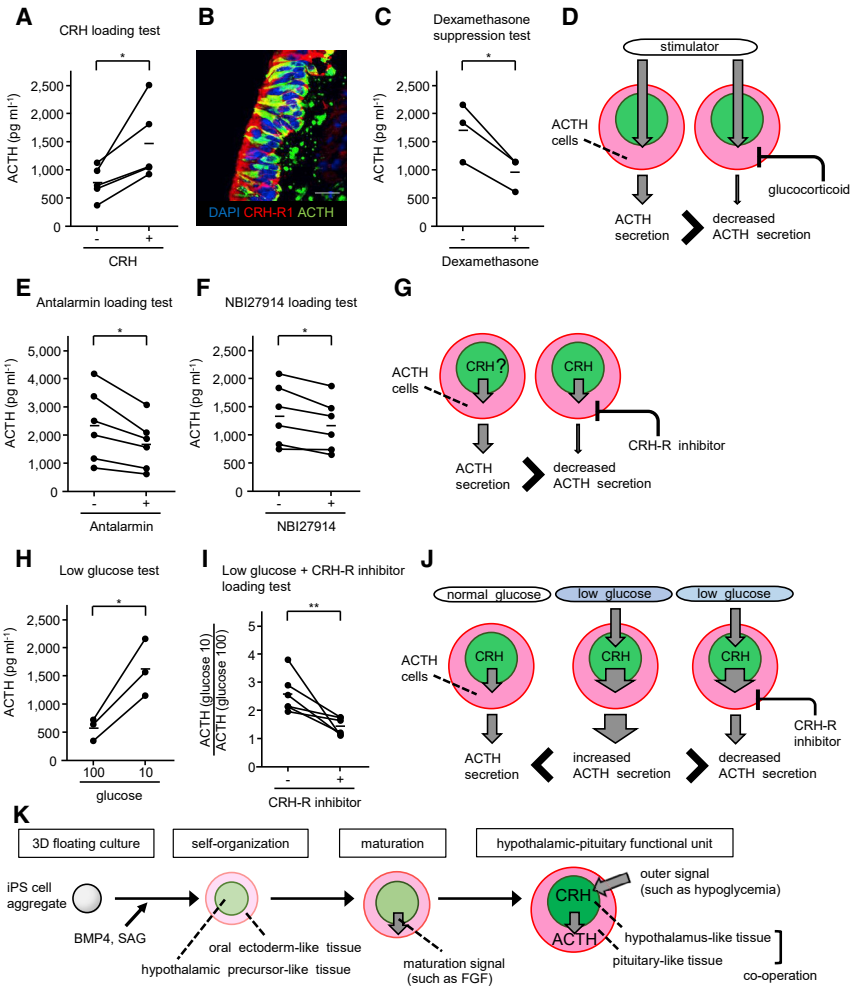

Figure 4. Functional Hypothalamic-Pituitary Axis in Hybrid Organoids

(A) CRH efficiently induced ACTH secretion (n = 5 experiments).

(B) All ACTH$^+$ cells expressed CRH-R1.

(C) Dexamethasone suppressed ACTH secretion (n = 3 experiments).

(D) Suppression of ACTH by glucocorticoid suggested that these aggregates retained negative feedback properties.

(E and F) CRH-R1 inhibitors (antalarmin or NBI27914) suppressed ACTH secretion (n = 6 experiments).

(G) Suppression of ACTH secretion by CRH-R1 inhibitors suggested that ACTH-positive cells functioned under the control of CRH-producing cells.

(H) Low glucose (10 mg/dL) stimulation induced ACTH secretion (n = 3 experiments).

(I) CRH inhibitor decreased elevation of ACTH secretion by low-glucose stimulation (n = 6 experiments).

(J) Change in ACTH in response to low-glucose stimulation or CRH-R1 inhibition suggested the stimulation by low glucose was transmitted through the CRH-ACTH pathway.

(K) Induction of differentiation into hypothalamic-pituitary functional units using human iPS cells.

Scale bars: 20 μm (B). Values shown in graphs represent means ± SEM. *$p < 0.05$, **$p < 0.01$, and ***$p < 0.001$.

medium (Figure 4H). This result suggests that pituitary ACTH$^+$ cells were under the control of the hypothalamus. Finally, we performed low-glucose stimulation after pretreatment with the CRH-R1 inhibitor. Although the ACTH increase in response to low-glucose stimulation was observed even when the CRH receptor 1 inhibitor was present, the degree of the increase was significantly smaller than when the CRH receptor 1 inhibitor was not added (Figure 4I). These data suggested that the stimulation by low glucose was transmitted through the CRH-ACTH pathway (Figure 4J). This result supports the idea that the anterior pituitary gland functioned under the control of the hypothalamus in our hybrid aggregates.

DISCUSSION

Several studies have induced pituitary cells from human pluripotent stem cells using two-dimensional adherent culture methods (Dincer et al., 2013; Zimmer et al., 2016). In contrast, we chose a 3D floating culture for our system. The advantage of our 3D culture is that anterior pituitary and hypothalamic neurons are juxtaposed similarly to the *in vivo* condition. Developmental biology has shown that the hypothalamus is important for induction and maturation of the anterior pituitary (Takuma et al., 1998; Rizzoti and Lovell-Badge, 2005; Zhu et al., 2007; Scully and Rosenfeld, 2002). The results of our study support this idea. We succeeded in generating mature hypothalamic tissue (hormone-positive neurons) by maintaining contact with pituitary tissues in continuous long-term culture. The coexistence of the hypothalamus and pituitary dramatically improved the ACTH secretion capacity and enabled regulation of ACTH by hypothalamic CRH. However, wide variation in the induction efficiency remains to be resolved in a future study.

One of the major problems in regenerative medicine has been that induced tissues are functionally inferior to normal tissues. For example, insulin secretion from induced pancreatic beta cells has been improved dramatically but still remains low (Pagliuca et al., 2014). In our method, human iPS cell-derived ACTH cells compared favorably with adult mice anterior pituitary cells, which represents an important benchmark in this field.

As a result of the juxtaposition of the pituitary and hypothalamus during the maturation stage, our aggregates acquired the ability to secrete ACTH in response to CRH in a self-regulating manner. *In vivo*, ACTH cells function under various types of regulation. One of the most important stimulants is hypothalamic CRH, whereas the inhibitory system is mediated by glucocorticoids (Vale et al., 1981; Keller-Wood and Dallman, 1984). Our aggregates responded appropriately to both regulators. Furthermore, investigations using CRH-R1 inhibitors have suggested that ACTH cells in a hybrid aggregate function under the control

of autonomous CRH cells. *In vivo*, hypothalamic hormones sense environmental information and regulate anterior pituitary hormones to strictly maintain homeostasis. The results of this study suggested that $ACTH^+$ cells functioned under the control of CRH^+ cells in the same hybrid aggregate. Therefore, we succeeded in simultaneously generating "hypothalamic-pituitary units" using human iPS cells (Figure 4K). Compared with the method for simple induction of the anterior pituitary, this hybrid induction method may reveal more complex relationships between tissues.

STAR★METHODS

Detailed methods are provided in the online version of this paper and include the following:

- KEY RESOURCES TABLE
- LEAD CONTACT AND MATERIALS AVAILABILITY
- EXPERIMENTAL MODEL AND SUBJECT DETAILS
  - Human iPS Cells
- METHOD DETAILS
  - Human iPS Cell Differentiation Culture
  - Immunohistochemistry
  - Quantitative PCR
  - ACTH Measurement in the Steady State
  - *In Vitro* Analysis of ACTH Release by a CRH Loading Test
  - *In Vitro* Analysis of ACTH Release by a Dexamethasone Loading Test
  - *In Vitro* Analysis of ACTH Release by a CRH Receptor Inhibitor Loading Test
  - *In Vitro* Analysis of ACTH Release by a Low Glucose Test
  - *In Vitro* Analysis of ACTH Release by a Low Glucose + CRH Receptor Inhibitor Loading Test
  - Electron Microscopy
  - Cell Immunoblot Assay (CIBA)
- QUANTIFICATION AND STATISTICAL ANALYSIS
- DATA AND CODE AVAILABILITY

SUPPLEMENTAL INFORMATION

Supplemental Information can be found online at https://doi.org/10.1016/j.celrep.2019.12.009.

ACKNOWLEDGMENTS

We are grateful to Takeshi Nigawara for the kind gift of the CRH-R1 antibody; Saishu Yoshida and Yukio Kato for technical guidance regarding rat pituitary primary culture; Jun Arita and Akira Shimatsu for instructions in the CIBA method; Masanori Suzuki for technical assistance regarding electron microscopy; Yasumasa Iwasaki, Yutaka Oki, Yutaka Takahashi, and Koji Takano for general advice; Tomiko Yamada, Akane Yasui, and Akiko Tsuzuki for technical support; and all members of the Arima laboratory for valuable discussions. We also thank Mitchell Arico from Edanz Group (https://www.edanzediting.com/ac) for editing a draft of this manuscript. This work was supported by grants from the Project for Technological Development (H.S.) of the Research Center Network for Realization of Regenerative Medicine (RCNRRM) and funded by the Japan Agency for Medical Research and Development (AMED), the Acceleration Program for Intractable Diseases Research Utilizing Disease-Specific iPS Cells (H.S.) of RCNRRM funded by AMED, grants-in-aid for scientific research (H.S.) from the Ministry of Education, Culture, Sports, Science and Technology of Japan (MEXT), and Nagoya University Hospital Funding for Clinical Research (H.S.).

AUTHOR CONTRIBUTIONS

T.K., H.S., C.O., R.M., and H.A. designed the study and wrote the manuscript. T.K., H.S., and M. Sakakibara performed the experiments with technical assistance and advice from M.K., K.M., K.O., Y.K., H.N., N.I., M. Sugiyama, T.O., T.T., Y.I., H.T., D.H., S.I., M.G., R.B., and J.T.

DECLARATION OF INTERESTS

The authors declare no competing interests.

Received: December 26, 2018
Revised: August 3, 2019
Accepted: December 3, 2019
Published: January 7, 2020

REFERENCES

Arita, J., Kojima, Y., and Kimura, F. (1993). Measurement of the secretion of a small peptide at the single cell level by the cell immunoblot assay: thyroidectomy increases the number of substance P-secreting anterior pituitary cells. Endocrinology *132*, 2682–2688.

Burman, P., Mattsson, A.F., Johannsson, G., Höybye, C., Holmer, H., Dahlqvist, P., Berinder, K., Engström, B.E., Ekman, B., Erfurth, E.M., et al. (2013). Deaths among adult patients with hypopituitarism: hypocortisolism during acute stress, and de novo malignant brain tumors contribute to an increased mortality. J. Clin. Endocrinol. Metab. *98*, 1466–1475.

Cooper, M.S., and Stewart, P.M. (2003). Corticosteroid insufficiency in acutely ill patients. N. Engl. J. Med. *348*, 727–734.

Dincer, Z., Piao, J., Niu, L., Ganat, Y., Kriks, S., Zimmer, B., Shi, S.H., Tabar, V., and Studer, L. (2013). Specification of functional cranial placode derivatives from human pluripotent stem cells. Cell Rep. *5*, 1387–1402.

Doi, D., Samata, B., Katsukawa, M., Kikuchi, T., Morizane, A., Ono, Y., Sekiguchi, K., Nakagawa, M., Parmar, M., and Takahashi, J. (2014). Isolation of human induced pluripotent stem cell-derived dopaminergic progenitors by cell sorting for successful transplantation. Stem Cell Reports *2*, 337–350.

Eiraku, M., Watanabe, K., Matsuo-Takasaki, M., Kawada, M., Yonemura, S., Matsumura, M., Wataya, T., Nishiyama, A., Muguruma, K., and Sasai, Y. (2008). Self-organized formation of polarized cortical tissues from ESCs and its active manipulation by extrinsic signals. Cell Stem Cell *3*, 519–532.

Hahner, S., Spinnler, C., Fassnacht, M., Burger-Stritt, S., Lang, K., Milovanovic, D., Beuschlein, F., Willenberg, H.S., Quinkler, M., and Allolio, B. (2015). High incidence of adrenal crisis in educated patients with chronic adrenal insufficiency: a prospective study. J. Clin. Endocrinol. Metab. *100*, 407–416.

Hoare, S.R., Sullivan, S.K., Ling, N., Crowe, P.D., and Grigoriadis, D.E. (2003). Mechanism of corticotropin-releasing factor type I receptor regulation by nonpeptide antagonists. Mol. Pharmacol. *63*, 751–765.

Keller-Wood, M.E., and Dallman, M.F. (1984). Corticosteroid inhibition of ACTH secretion. Endocr. Rev. *5*, 1–24.

Nakamura, M., and Okano, H. (2013). Cell transplantation therapies for spinal cord injury focusing on induced pluripotent stem cells. Cell Res. *23*, 70–80.

Nigawara, T., Horiba, N., Tozawa, F., Kasagi, Y., Uchida, K., Iwasaki, Y., and Suda, T. (2003). Regulation of corticotropin releasing hormone receptor (CRH-R) in the rat anterior pituitary as assessed by radioimmunoassay. Pituitary *6*, 67–73.

Ogawa, K., Suga, H., Ozone, C., Sakakibara, M., Yamada, T., Kano, M., Mitsumoto, K., Kasai, T., Kodani, Y., Nagasaki, H., et al. (2018). Vasopressin-secreting neurons derived from human embryonic stem cells through specific induction of dorsal hypothalamic progenitors. Sci. Rep. *8*, 3615.

Ozone, C., Suga, H., Eiraku, M., Kadoshima, T., Yonemura, S., Takata, N., Oiso, Y., Tsuji, T., and Sasai, Y. (2016). Functional anterior pituitary generated in self-organizing culture of human embryonic stem cells. Nat. Commun. *7*, 10351.

Pagliuca, F.W., Millman, J.R., Gürtler, M., Segel, M., Van Dervort, A., Ryu, J.H., Peterson, Q.P., Greiner, D., and Melton, D.A. (2014). Generation of functional human pancreatic β cells *in vitro*. Cell *159*, 428–439.

Perrin, M.H., and Vale, W.W. (1999). Corticotropin releasing factor receptors and their ligand family. Ann. N Y Acad. Sci. *885*, 312–328.

Plotsky, P.M., Bruhn, T.O., and Vale, W. (1985). Hypophysiotropic regulation of adrenocorticotropin secretion in response to insulin-induced hypoglycemia. Endocrinology *117*, 323–329.

Rizzoti, K., and Lovell-Badge, R. (2005). Early development of the pituitary gland: induction and shaping of Rathke's pouch. Rev. Endocr. Metab. Disord. *6*, 161–172.

Schwartz, S.D., Tan, G., Hosseini, H., and Nagiel, A. (2016). Subretinal transplantation of embryonic stem cell-derived retinal pigment epithelium for the treatment of macular degeneration: an assessment at 4 years. Invest. Ophthalmol. Vis. Sci. *57*, ORSFc1-9.

Scully, K.M., and Rosenfeld, M.G. (2002). Pituitary development: regulatory codes in mammalian organogenesis. Science *295*, 2231–2235.

Sherlock, M., Ayuk, J., Tomlinson, J.W., Toogood, A.A., Aragon-Alonso, A., Sheppard, M.C., Bates, A.S., and Stewart, P.M. (2010). Mortality in patients with pituitary disease. Endocr. Rev. *31*, 301–342.

Stewart, P.M., Biller, B.M., Marelli, C., Gunnarsson, C., Ryan, M.P., and Johannsson, G. (2016). Exploring inpatient hospitalizations and morbidity in patients with adrenal insufficiency. J. Clin. Endocrinol. Metab. *101*, 4843–4850.

Suga, H., Kadoshima, T., Minaguchi, M., Ohgushi, M., Soen, M., Nakano, T., Takata, N., Wataya, T., Muguruma, K., Miyoshi, H., et al. (2011). Self-formation of functional adenohypophysis in three-dimensional culture. Nature *480*, 57–62.

Takuma, N., Sheng, H.Z., Furuta, Y., Ward, J.M., Sharma, K., Hogan, B.L., Pfaff, S.L., Westphal, H., Kimura, S., and Mahon, K.A. (1998). Formation of Rathke's pouch requires dual induction from the diencephalon. Development *125*, 4835–4840.

Vale, W., Spiess, J., Rivier, C., and Rivier, J. (1981). Characterization of a 41-residue ovine hypothalamic peptide that stimulates secretion of corticotropin and beta-endorphin. Science *213*, 1394–1397.

Vermes, I., Beishuizen, A., Hampsink, R.M., and Haanen, C. (1995). Dissociation of plasma adrenocorticotropin and cortisol levels in critically ill patients: possible role of endothelin and atrial natriuretic hormone. J. Clin. Endocrinol. Metab. *80*, 1238–1242.

Webster, E.L., Lewis, D.B., Torpy, D.J., Zachman, E.K., Rice, K.C., and Chrousos, G.P. (1996). *In vivo* and *in vitro* characterization of antalarmin, a nonpeptide corticotropin-releasing hormone (CRH) receptor antagonist: suppression of pituitary ACTH release and peripheral inflammation. Endocrinology *137*, 5747–5750.

Zhu, X., Gleiberman, A.S., and Rosenfeld, M.G. (2007). Molecular physiology of pituitary development: signaling and transcriptional networks. Physiol. Rev. *87*, 933–963.

Zimmer, B., Piao, J., Ramnarine, K., Tomishima, M.J., Tabar, V., and Studer, L. (2016). Derivation of Diverse Hormone-Releasing Pituitary Cells from Human Pluripotent Stem Cells. Stem Cell Reports *6*, 858–872.

STAR★METHODS

KEY RESOURCES TABLE

REAGENT or RESOURCE	SOURCE	IDENTIFIER
Antibodies		
RX	This paper	N/A
pan-cytokeratin	Sigma-Aldrich	C2562; RRID: AB_476839
LHX3	This paper	N/A
PITX1	This paper	N/A
NKX2.1	Zymed	18-0221; RRID: AB_86728
E-cadherin	Takara	M108
ACTH	Fitzgerald	10C-CR1096M1; RRID: AB_1282437
CRH	Santa Cruz Biotechnology	sc-1759; RRID: AB_631300
CRH-R1	This paper	N/A
AVP	Peninsula	T-5048; RRID: AB_2313978
oxytocin	Millipore	MAB5296; RRID: AB_2157626
AGRP	Neuromics	GT15023; RRID: AB_2687600
POMC	Abcam	ab14064; RRID: AB_300892
MCH	Sigma-Aldrich	M8440; RRID: AB_260690
TRH	Sigma-Aldrich	HPA035595; RRID: AB_10669525
NPY	Abcam	Ab30914; RRID: AB_1566510
GHRH	Bioss	bs-0205R; RRID: AB_10856019
FGF8	R&D	MAB323; RRID: AB_2102956
FGF10	PeproTec	500-P151; RRID: AB_148138
ACTH for immunoelectron microscopy	DAKO	M3501; RRID: AB_2166039
Colloidal Gold Conjugated Goat Purified Antibody To Mouse IgG	Sigma-Aldrich	G7652; RRID: AB_259958
488 donkey anti-mouse	Life Technology	A21202; RRID: AB_141607
488 goat anti- Guinea Pig	Life Technology	A11073; RRID: AB_2534117
546 donkey anti-goat	Life Technology	A11056; RRID: AB_2534103
546 donkey anti-rabbit	Life Technology	A10040; RRID: AB_2534016
546 donkey anti-mouse	Life Technology	A10036; RRID: AB_2534012
546 goat anti-chicken	Life Technology	A11040; RRID: AB_2534097
546 goat anti-Guinea Pig	Life Technology	A11074; RRID: AB_2534118
647 goat anti-rat	Life Technology	A21247; RRID: AB_141778
Cy3 donkey anti Guinea Pig	Jackson	706-165-148; RRID: AB_2340460
Chemicals, Peptides, and Recombinant Proteins		
DMEM-F12	Sigma-Aldrich	D6421
non-essential amino acids	Thermo Fisher	11140050
L-glutamine	Thermo Fisher	25030081
KSR	Thermo Fisher	10828028
2-mercaptoethanol	Wako	131-14572; CAS: 60-24-2
recombinant human basic FGF	Wako	068-04544
trypsin	Difco	215240
collagenase type IV	Thermo Fisher	17104019
TrypLE Express	Thermo Fisher	12605010
DNase I	Roche	1284932
Y-27632	Wako	034-24024; CAS: 331752-47-7
V-bottom 96-well plate	Sumitomo Bakelite	MS-9096V
Iscove's modified Dulbecco's medium	Thermo Fisher	31980097

(*Continued on next page*)

Continued

REAGENT or RESOURCE	SOURCE	IDENTIFIER
Ham's F12	Thermo Fisher	31765092
chemically defined lipid concentrate	Thermo Fisher	11905031
1-thioglycerol	Sigma-Aldrich	M6145; CAS: 96-27-5
bovine serum albumin	Sigma-Aldrich	A3156; CAS: 9048-46-8
BMP4	R&D	314-BP
SAG	Cayman	11914; CAS: 912545-86-9
EZ sphere	IWAKI	4020-900
sodium hydrogen carbonate	Sigma-Aldrich	28-1805-5
penicillin/streptomycin	Thermo Fisher	15140122
N2 supplement	Thermo Fisher	17502048
B27 supplement	Thermo Fisher	12587010
recombinant human CNTF	R&D	257-NT
human CRH	Tanabe	7223406D1030
dexamethasone	Aspen	2454405H1024
Antalarmin	Sigma-Aldrich	A8727; CAS: 220953-69-5
NBI27914	Sigma-Aldrich	N3911; CAS: 184241-44-9
D-glucose	Sigma-Aldrich	G8270; CAS: 50-99-7
D-mannitol	Sigma-Aldrich	M9546; CAS: 69-65-8
DMEM without glucose	Thermo Fisher	11966025
HBSS	Thermo Fisher	14025092
Collagenase type I	Wako	037-17603; CAS: 9001-12-1
0.25% trypsin/EDTA	Wako	201-16945
40 μm cell strainer	Falcon	352340
Polyvinylidene difluoride transfer membrane	Millipore	ISEQ09120
methanol	Wako	131-01826; CAS: 67-56-1
EBSS	Sigma-Aldrich	E3024
slide glass	Matsunami	S9441
small glass coverslips	Matsunami	C018241
large glass coverslip	Matsunami	C024601
human ACTH	GenScript	RP11304; CAS: 12279-41-3
TBS	Sigma-Aldrich	T5912
1-μl microsyringe	Ito Manufactory	MS-01
plastic capillary	Drummond Scientific	8-000-7520/5
4% paraformaldehyde in 0.1 M phosphate buffer	Wako	163-20145; CAS: 30525-89-4
sheep serum	Sigma-Aldrich	S3772
biotinylated anti–mouse IgG	GE Healthcare	RPN1001
streptavidin–alkaline phosphatase conjugate	GE Healthcare	RPN1234
1-step NBT/BCIP suppressor substrate solution	Thermo Fisher	34070
PD-173074	Millipore	341607
DAPI	Dojindo	D212
RNeasy kit	QIAGEN	74106
DNase	QIAGEN	79254
Power SYBR Green PCR Master Mix	Thermo Fisher	4367659
Experimental Models: Cell Lines		
201B7	RIKEN BRC	RBRC-HPS0063
409B2	RIKEN BRC	RBRC-HPS0076
454E2	RIKEN BRC	RBRC-HPS0077

(*Continued on next page*)

Continued

REAGENT or RESOURCE	SOURCE	IDENTIFIER
Oligonucleotides		
Forward primer for GAPDH: 5′-GAGTCAACGGATTTGGTCGT-3′	This paper	N/A
Reverse primer for GAPDH: 5′-TTGATTTTTGGAGGGATCTCCG-3′	This paper	N/A
Forward primer for LHX3: 5′-GGCTGGCCTGTGTGTAAGTC-3′	This paper	N/A
Reverse primer for LHX3: 5′-CATTCACAGAACCAATAGGTAGCTC-3′	This paper	N/A
Forward primer for POMC: 5′-GAAGATGCCGAGATCGTGCT-3′	This paper	N/A
Reverse primer for POMC: 5′-ACGTACTTCCGGGGGTTCTC-3′	This paper	N/A
Software and Algorithms		
cellSens imaging software	Olympus	https://www.olympus-lifescience.com/en/software/cellsens/#!

LEAD CONTACT AND MATERIALS AVAILABILITY

Further information and requests for resources and reagents should be directed to and will be fulfilled by the Lead Contact, Hidetaka Suga (sugahide@med.nagoya-u.ac.jp). All reagents generated in this study are available from the Lead Contact with a completed Materials Transfer Agreement.

EXPERIMENTAL MODEL AND SUBJECT DETAILS

Human iPS Cells

Human iPS cell lines (201B7, 409B2, and 454E2) were established from female cells and provided by RIKEN BRC. For maintenance culture, iPS cells were cultured on mitomycin C-treated mouse embryonic fibroblasts as feeder cells. The maintenance medium consisted of DMEM-F12, 0.1 mM non-essential amino acids, 2 mM L-glutamine, 20% KSR, 0.1 mM 2-mercaptoethanol, and 5 ng/ml recombinant human basic FGF. Passaging was performed every 6–8 days at split ratios of 1:3–1:5 using a dissociation solution consisting of 0.25% trypsin, 1 mg/ml collagenase type IV, 20% KSR, and 1 mM $CaCl_2$ in PBS.

METHOD DETAILS

Human iPS Cell Differentiation Culture

The SFEBq method was used for differentiation culture. Human iPS cells were dissociated into single cells using TrypLE Express containing 0.067 mg/ml DNase I and 67 μM Y-27632, and then seeded in a V-bottom 96-well plate. Differentiation medium was growth factor-free Chemically Defined Medium (gfCDM) plus a fixed concentration of KSR. gfCDM consisted of Iscove's modified Dulbecco's medium/Ham's F12 (1:1), 1% chemically defined lipid concentrate, 450 μM 1-thioglycerol, and 5 mg/ml purified bovine serum albumin (BSA). The culture start date was defined as day 0.

On day 0, 5,000 human iPS cells were seeded in 100 μL differentiation medium (gfCDM + 5% KSR) in each well. Y-27632 was added at a concentration of 20 μM. On day 3, 100 μL differentiation medium was added to each well. From day 6 to 27, half of the differentiation medium was replaced every 3 days. From day 6, BMP4 and SAG were added at final concentrations of 5 nM and 2 μM, respectively. After 18, BMP4 was not added, and the concentration decreased gradually. The concentration of SAG was maintained at 2 μM even after day 18. From day 18, the culture was maintained in a high oxygen concentration (40%). On day 30, aggregates were collected from 96-well plates and transferred to an EZ sphere. From day 30, the differentiation medium was changed to gfCDM + 10% KSR. SAG continued to be added at the same concentration even after day 30. From day 33, the differentiation medium was completely replaced every 3 days. From day 51, the differentiation medium was switched to gfCDM + 20% KSR. This method is based on a previous report describing differentiation culture of human ES cells. Efforts to improve the differentiation efficiency focused on varying the following parameters (as described in the main text and figures): number of cells per well, KSR concentration, BMP4 concentration, SAG concentration, and timing of BMP4 and SAG addition.

In Figures 3J–3L, to prepare the DFNB medium, the DFG medium was first prepared by adding 500 mL DMEM-F12, 3.85 g glucose, 1.2 g sodium hydrogen carbonate and 5 mL penicillin/streptomycin to MilliQ water. The pH was adjusted to 7.6. DFNB medium was

prepared by combining 485 mL DFG medium, 5 mL of 1 × N2 supplement, 10 mL of 1 × B27 supplement, and 5 μL of recombinant human CNTF. Recombinant human CNTF was reconstitute at 0.1 μg/μL in filtered PBS (-) containing 0.1% BSA.

Immunohistochemistry

Samples were incubated with primary antibodies (Key resource table) overnight at 4°C and then with secondary antibodies (Key resource table) for 2 hours at room temperature. Primary antibodies were applied at the following dilutions: RX (1:3000), pan-cytokeratin (1:100), LHX3 (1:3000), PITX1 (1:2000), NKX2.1 (1:1000), E-cadherin (1:50), ACTH (1:200), CRH (1:100), AVP (1:2000), oxytocin (1:100), AGRP (1:250), POMC (1:200), MCH (1:500), TRH (1:1000), NPY (1:1000), GHRH (1:100), FGF8 (1:100), and FGF10 (1:100). The antiserum against RX was raised in guinea pigs using the synthetic peptide FTKDDGILGTFPAERGARGAKERDRRLGARPACPKA-PEEGSEPSPPPAPAPAPEYEAPRPYCPKEPWEARPSPGLPVGPATGEAKLSEEE (N-terminal, 90 residues). The antiserum against LHX3 was raised in guinea pigs using the synthetic peptide C-PSSDLSTGSSGGYPDFPASPASWLDEVDHAQF (residues 366–397). The antiserum against PITX1 was raised in guinea pigs using the synthetic peptide DPREPLENSASESSDTELPEKERGGEPKG-PEDSGAGGTG-C (residues 38–77). DAPI was used to counterstain nuclei. Differential induction efficiency was calculated by measuring the number of $LHX3^+$ cells or $ACTH^+$ cells and dividing that value by the number of $DAPI^+$ cells in the aggregate as a whole. The cutoff in Figures S2A, S2B, and S4A was whether positive cells were included in the section with the maximum diameter.

Quantitative PCR

Quantitative PCR (qPCR) was performed on five or six aggregates per sample. RNAs were purified using RNeasy kit after treatment with DNase. qPCR was performed using Power SYBR Green PCR Master Mix and analyzed with the MX3000P system. Data were normalized against the corresponding levels of GAPDH mRNA. Primers are shown in the Key resource table.

ACTH Measurement in the Steady State

To assess autonomous secretion of ACTH from iPS cell-derived aggregates, we measured the ACTH concentration in conditioned medium in the steady state. A full medium change (10ml per 30 aggregates) was performed and the culture supernatant was collected after 24 hours of culture at 37°C. The collected culture supernatant was immediately frozen at −180°C and analyzed using electro chemiluminescence immunoassay (ECLIA) kit (SRL), which is used clinically in Japan. The baseline ACTH values of the culture medium without any aggregates (negative control) was 4.8 ± 0.12 pg/mL.

In Vitro Analysis of ACTH Release by a CRH Loading Test

A CRH loading test was performed on days 113–152. Eight to 16 aggregates were used for the test. A full medium change was performed with gfCDM + 20% KSR + 2 μM SAG, and the culture supernatant was collected after 24 hours of culture at 37°C. The ACTH values in culture supernatant were measured. Then, another full medium change was performed with gfCDM + 20% KSR + 2 μM SAG + human CRH (5 μg/ml), and the culture supernatant was collected again after 24 hours of culture at 37°C. The ACTH values in the culture supernatants were measured as described above.

In Vitro Analysis of ACTH Release by a Dexamethasone Loading Test

A CRH loading test was performed on days 141–229. Eight to 34 aggregates were used for the test. A full medium change was performed with gfCDM + 20% KSR + 2 μM SAG, and the culture supernatant was collected after 24 hours of culture at 37°C. Then, another full medium change was performed with gfCDM + 20% KSR + 2 μM SAG + dexamethasone (500 ng/ml), and the culture supernatant was collected again after 24 hours of culture at 37°C.

In Vitro Analysis of ACTH Release by a CRH Receptor Inhibitor Loading Test

An antalarmin loading test was performed on days 193–273. Eight to 35 aggregates per group were used for the test. A full medium change was performed with gfCDM + 20% KSR + 2 μM SAG, and the culture supernatant was collected after 24 hours of culture at 37°C. Then, another full medium change was performed with gfCDM + 20% KSR + 2 μM SAG + antalarmin (1×10^{-5} M), and the culture supernatant was collected again after 24 hours of culture at 37°C.

An NBI27914 loading test was performed on days 163–243. Eight to 35 aggregates were used for the test. The NBI27914 loading test was performed similarly to the antalarmin loading test using an NBI27914 concentration of 1×10^{-5} M.

In Vitro Analysis of ACTH Release by a Low Glucose Test

A low glucose test was performed on days 192–240. Ten to 20 aggregates for each group were used for the test. To apply low glucose stimulation to the hypothalamus portion inside the aggregate, the aggregates were cut into several pieces a few days before the experiment. Low glucose medium (10 mg/dl glucose) was prepared by adding 0.56 mM D-glucose and 9.44 mM D-mannitol to DMEM without glucose. Normal glycemic medium (100 mg/dl glucose) was prepared by adding 5.56 mM D-glucose and 4.44 mM D-mannitol to DMEM without glucose. The culture supernatant was collected at 30 minutes after the medium was replaced with normal glycemic medium, and then again at 30 minutes after the medium was replaced with low glucose medium. The ACTH values in culture supernatant samples were compared.

In Vitro Analysis of ACTH Release by a Low Glucose + CRH Receptor Inhibitor Loading Test

A low glucose + CRH-R inhibitor loading test was performed on days 222–270. Ten to 20 aggregates were used for the test. For the low glucose test, ACTH secretion was confirmed in response to low glucose without the CRH receptor inhibitor, and then the medium was replaced with gfCDM + 20% KSR + 2 μM SAG + antalarmin (1×10^{-5} M) + NBI 27914 (1×10^{-5} M), followed by overnight culture. Then, low glucose medium and normal glucose medium containing both antalarmin (1×10^{-5} M) and NBI 27914 (1×10^{-5} M) were prepared, and secretion of ACTH was confirmed as described for the low glucose test. The ACTH values in the culture supernatants were compared.

Electron Microscopy

To prepare specimens for electron microscopy, aggregates were fixed in 2.5% glutaraldehyde for 3 days at 4°C and postfixed in 1% osmium tetraoxide for 1 hour. The tissue block was dehydrated in a graded series of alcohol solutions and embedded in Epon 812. Semithin sections of the tissue blocks stained with toluidine blue. Ultrathin sections were then prepared, stained with 2% uranyl acetate and 0.2% lead citrate, and examined under a Hitachi H-7500 electron microscope.

For immunoelectron microscopy, the sections were pretreated with $NaIO_4$ and 10% hydrogen peroxide in ethanol. After etching, they were incubated with a 1:2000 dilution of a mouse monoclonal antibody against ACTH for 1 hour at 37°C. After incubation, the sections were washed with PBS and then incubated with a 1:10 dilution of mouse IgG conjugated with 10 nm gold particles for 1 hour at 37°C.

Cell Immunoblot Assay (CIBA)

The CIBA was based on the method of Arita et al. with some modifications First, aggregates that had undergone pituitary differentiation for 150 days were dispersed into single cells. The mouse pituitary gland was similarly dispersed into single cells. Minced tissue was washed in HBSS and incubated for 40 minutes at 37°C in a solution containing 0.2% collagenase type I and 20 μM Y-27632 in HBSS. The fragments were washed in PBS and further incubated at 37°C in a solution containing 0.25% trypsin/EDTA, 67 μM Y-27632, and 0.2 mg/ml DNase I for 10 minutes. After gfCDM + 20% KSR was added, the fragments were centrifuged for 5 minutes at 100 × *g*. The fragments were triturated with a pipette in medium consisted of gfCDM with 20% KSR, 20 μM Y-27632, and 0.01 mg/ml DNase I until the cells were monodispersed. The dispersed cells were passed through a cell strainer (40 μm) and suspended at a density of 6×10^5 cells/ml.

A polyvinylidene difluoride membrane was cut to 5.2 × 2.2 cm, soaked in methanol for 20 s, and then washed in EBSS containing 20 mM HEPES for 60 minutes. The membrane was then placed on a slide glass. Two small glass coverslips (18 × 24 mm) were placed on the membrane at approximately 20 mm apart. One large glass coverslip (60 × 24 mm) was placed on a small glass coverslip and used as the ceiling of the chamber. The incubation chamber had an average volume of 54 μl.

One hundred microliters of cell suspension was poured into the incubation chamber. To prevent drying, the chambers were placed in a water-tight plastic box and then cultured at 37°C in a 5% CO_2 air incubator for 21 hours. As a standard for quantitation, various amounts (0–500 pg) of human ACTH were dissolved in 50 nL TBS containing 0.8% Tween-20, spotted on a transfer membrane with a 1 μL microsyringe and plastic capillary, and incubated in the same manner as the cells. After incubation, the coverslips were removed in PBS, the membrane was soaked in 10% BSA/PBS, and surplus portions of the membrane were removed. Membranes were incubated in 10% BSA/PBS for 20 minutes, washed three times with 0.1 M phosphate buffer for 3 minutes, fixed with 4% paraformaldehyde in 0.1 M phosphate buffer for 10 minutes, washed three times with TBS for 10 minutes, and then blocked with 10% BSA in TBS for 2 hours. Membranes were incubated in 10% normal sheep serum in solution A (500 mM NaCl, 50 mM Tris, 0.5% Tween-20, 1% BSA, and NaN_3) for 30 minutes, and then in mouse anti-ACTH (1:1000) in 10% normal sheep serum in solution A overnight, followed by incubation with biotinylated anti-mouse IgG (1:500) in 10% normal sheep serum in solution A for 40 minutes and then in streptavidin-alkaline phosphatase conjugate (1:3000) in solution A for 40 minutes. After each incubation, membranes were washed with TBS containing 0.1% Tween-20 for 20 minutes. Membranes were incubated in 1-step NBT/BCIP suppressor substrate solution containing 5 mM $MgCl_2$ for 3 minutes, washed with distilled water for 15 minutes, dried, and then evaluated.

Evaluation was performed using a BX63 microscope and cellSens imaging software. Ten fields of view were chosen randomly, and the density of the blot in the field of view was measured. The average density of the background around the blot was measured and subtracted from the density of the blot. The amount of ACTH secretion was calculated based on a standard curve created using the spots of ACTH standard solution, multiplying the density level by the area for each concentration.

QUANTIFICATION AND STATISTICAL ANALYSIS

Statistical analyses were performed with GraphPad Prism 6.0 software. Data are expressed as means ± s.e.m. Comparisons between two groups were performed by the Student's t test. Comparisons between multiple groups were performed by the one-way ANOVA test with post hoc Bonferroni's method. n refers to number of independent experiments. Each experiment was done in a different batch. P values of < 0.05 (*), < 0.01 (**), < 0.001 (***) were considered significant. P values are indicated in figure legends.

DATA AND CODE AVAILABILITY

This study did not generate/analyze datasets or code.

Cell Reports, Volume *30*

Supplemental Information

Hypothalamic Contribution to Pituitary Functions Is Recapitulated *In Vitro* Using 3D-Cultured Human iPS Cells

Takatoshi Kasai, Hidetaka Suga, Mayu Sakakibara, Chikafumi Ozone, Ryusaku Matsumoto, Mayuko Kano, Kazuki Mitsumoto, Koichiro Ogawa, Yu Kodani, Hiroshi Nagasaki, Naoko Inoshita, Mariko Sugiyama, Takeshi Onoue, Taku Tsunekawa, Yoshihiro Ito, Hiroshi Takagi, Daisuke Hagiwara, Shintaro Iwama, Motomitsu Goto, Ryoichi Banno, Jun Takahashi, and Hiroshi Arima

Figure S1

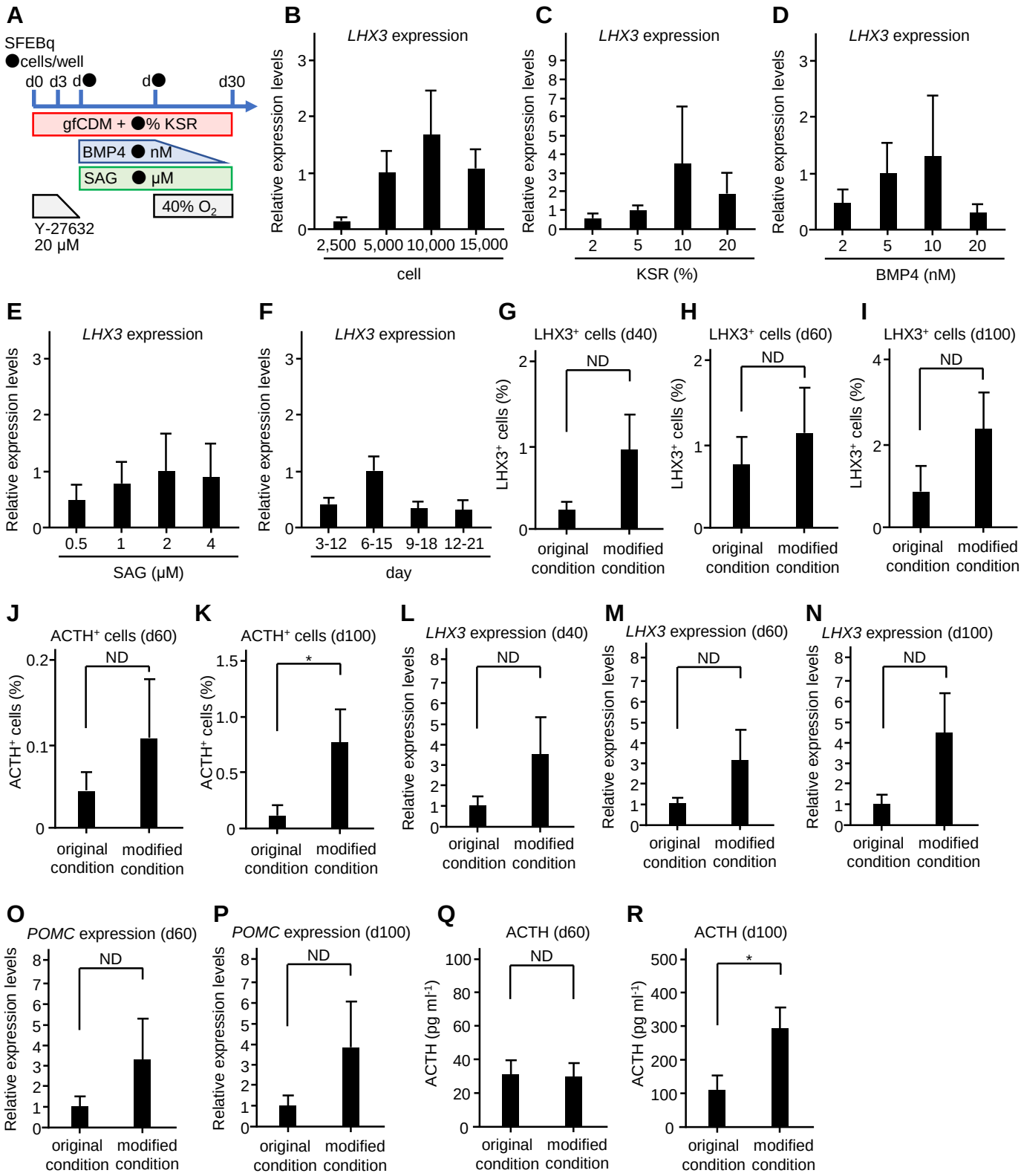
A
SFEBq
●cells/well
d0 d3 d● d● d30
gfCDM + ●% KSR
BMP4 ● nM
SAG ● μM
40% O2
Y-27632
20 μM
B
LHX3 expression
Relative expression levels
2,500 5,000 10,000 15,000
cell
C
LHX3 expression
Relative expression levels
2 5 10 20
KSR (%)
D
LHX3 expression
Relative expression levels
2 5 10 20
BMP4 (nM)
E
LHX3 expression
Relative expression levels
0.5 1 2 4
SAG (μM)
F
LHX3 expression
Relative expression levels
3-12 6-15 9-18 12-21
day
G
LHX3+ cells (d40)
LHX3+ cells (%)
ND
original condition
modified condition
H
LHX3+ cells (d60)
LHX3+ cells (%)
ND
original condition
modified condition
I
LHX3+ cells (d100)
LHX3+ cells (%)
ND
original condition
modified condition
J
ACTH+ cells (d60)
ACTH+ cells (%)
ND
original condition
modified condition
K
ACTH+ cells (d100)
ACTH+ cells (%)
*
original condition
modified condition
L
LHX3 expression (d40)
Relative expression levels
ND
original condition
modified condition
M
LHX3 expression (d60)
Relative expression levels
ND
original condition
modified condition
N
LHX3 expression (d100)
Relative expression levels
ND
original condition
modified condition
O
POMC expression (d60)
Relative expression levels
ND
original condition
modified condition
P
POMC expression (d100)
Relative expression levels
ND
original condition
modified condition
Q
ACTH (d60)
ACTH (pg ml-1)
ND
original condition
modified condition
R
ACTH (d100)
ACTH (pg ml-1)
*
original condition
modified condition

Figure S1. Additional data of the modified condition using 201B7. Related to Figure 1.

(A–F) Optimization of the modified condition.
(A) Culture parameters that were changed.
(B–F) Expression of LHX3 on day 40 in response to modification of each culture parameter (qPCR; n = 3 experiments).

(G–K) Proportion of $LHX3^+$ cells and $ACTH^+$ cells as determined by immunostaining (day 40 and 60, n = 14 experiments; day 100, n = 12 experiments).
(L–P) Expression of LHX3 and POMC as determined by qPCR (day 40 and 60, n = 14 experiments; day 100, n = 12 experiments).
(Q, R) ACTH values in the culture medium (day 60, n = 14 experiments; day 100, n = 20 experiments).

Values shown on graphs represent means ± s.e.m. *P<0.05

Figure S2

A

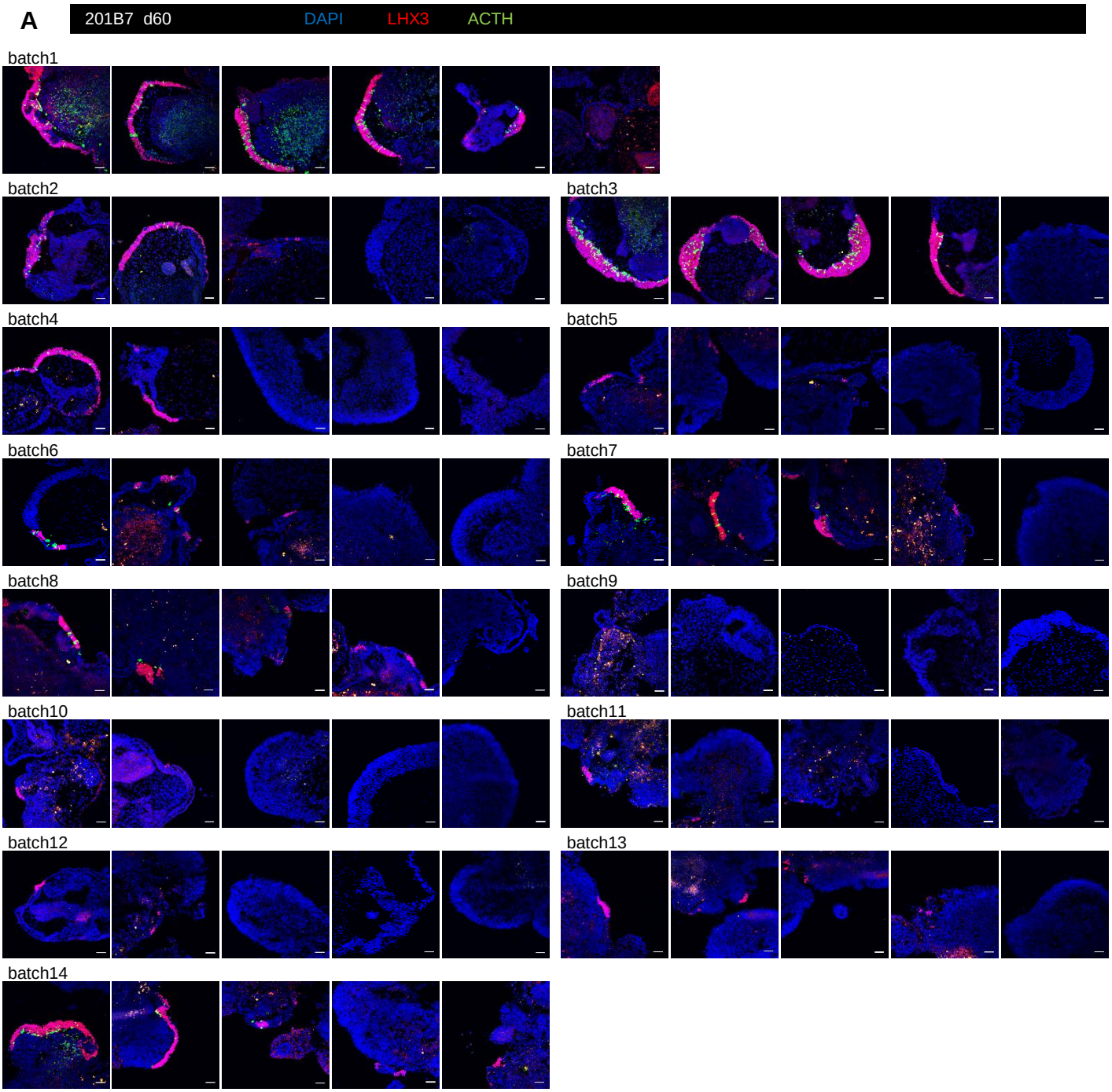

B

Batch number	Number of aggregates containing both LHX3⁺ cells and ACTH⁺ cells	Number of aggregates containing LHX3⁺ cells	Total number of aggregates	ACTH concentration in culture supernatants (pg/ml)
1	5	6	6	119.0
2	2	3	5	9.1
3	4	4	5	72.8
4	1	2	5	13.7
5	0	3	5	14.2
6	2	3	5	21.4
7	3	4	5	37.5
8	2	4	5	30.5
9	0	1	5	12.4
10	0	2	5	12.9
11	0	3	5	16.9
12	0	2	5	13.7
13	0	4	5	21.4
14	3	5	5	18.9
total	22	46	71	

Figure S2. Expression of LHX3 and ACTH in day 60 aggregates cultured under the modified condition. Related to Figure 1.

(A-B) Additional data of Figures S1H and S1J.
(A) 201B7 cells were cultured under the modified condition. Aggregates were evaluated on day 60. All immunostaining images are shown. The cutoff was whether positive cells were included in the section with the largest diameter.
(B) Number of aggregates containing both $LHX3^+$ cells and $ACTH^+$ cells in each batch. About 30% (22/71 aggregates) of the aggregates contained both $LHX3^+$ cells and $ACTH^+$ cells. About 60% (46/71) of the aggregates contained $LHX3^+$ cells. Even among the aggregates determined to be negative ACTH, many aggregates contained $LHX3^+$ cells, indicating that they were pituitary precursor cells. The rightmost column shows the amount of ACTH secretion on day 60 (30 aggregates in 10 ml culture medium). The baseline ACTH values of the culture medium without any aggregates (negative control) was 4.8 ± 0.12 pg/mL. These data suggest that even batches defined as negative for ACTH by this criterion may contain differentiated ACTH cells.

Scale bars: 50μm (A).

Figure S3

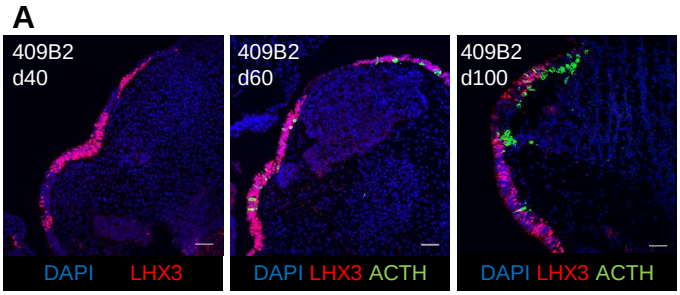
A
409B2 d40
409B2 d60
409B2 d100
DAPI LHX3
DAPI LHX3 ACTH

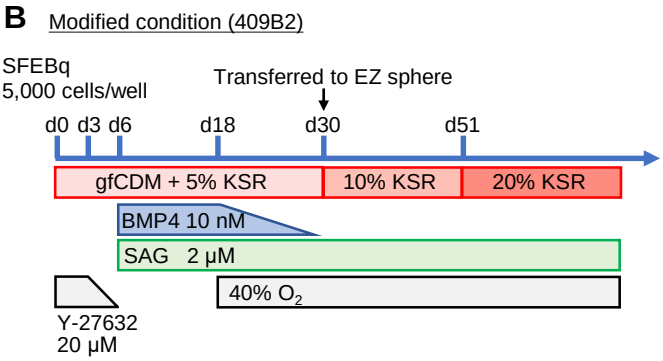
B
Modified condition (409B2)
SFEBq
5,000 cells/well
Transferred to EZ sphere
d0 d3 d6 d18 d30 d51
gfCDM + 5% KSR
10% KSR
20% KSR
BMP4 10 nM
SAG 2 μM
40% O2
Y-27632
20 μM

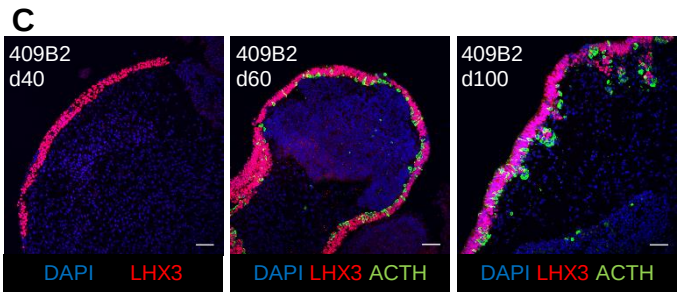
C
409B2 d40
409B2 d60
409B2 d100
DAPI LHX3
DAPI LHX3 ACTH

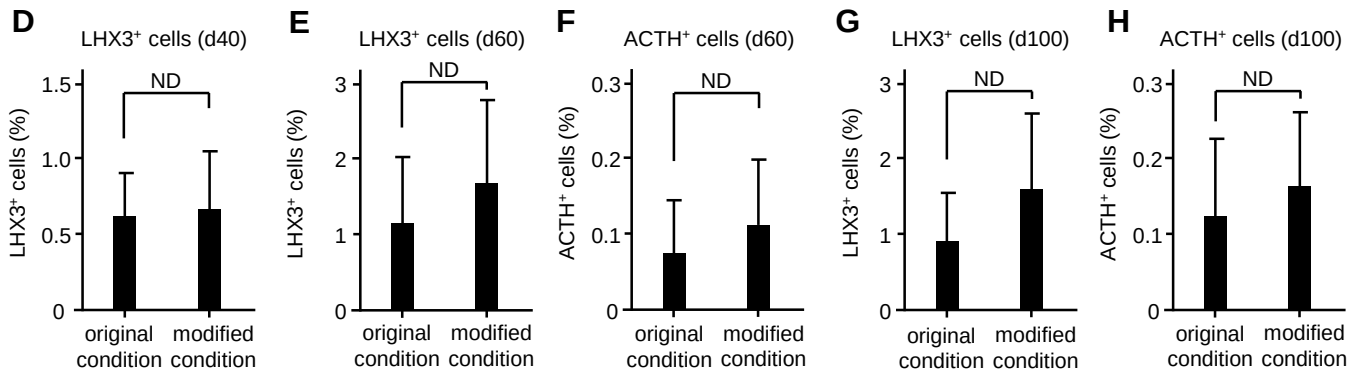
D
LHX3+ cells (d40)
E
LHX3+ cells (d60)
F
ACTH+ cells (d60)
G
LHX3+ cells (d100)
H
ACTH+ cells (d100)
ND
LHX3+ cells (%)
ACTH+ cells (%)
original condition
modified condition

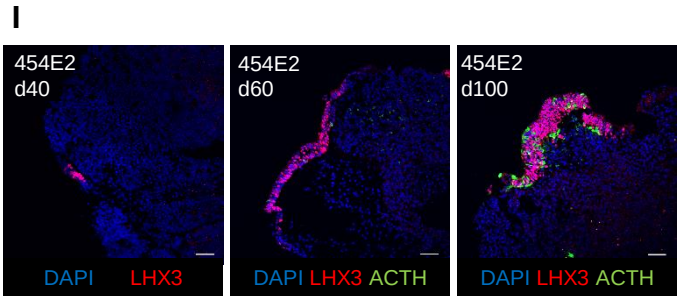
I
454E2 d40
454E2 d60
454E2 d100
DAPI LHX3
DAPI LHX3 ACTH

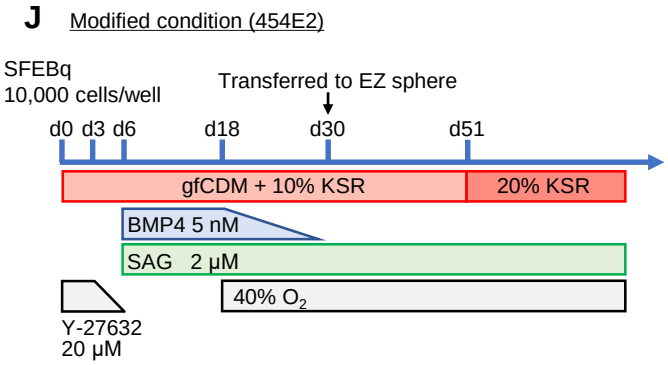
J
Modified condition (454E2)
SFEBq
10,000 cells/well
Transferred to EZ sphere
d0 d3 d6 d18 d30 d51
gfCDM + 10% KSR
20% KSR
BMP4 5 nM
SAG 2 μM
40% O2
Y-27632
20 μM

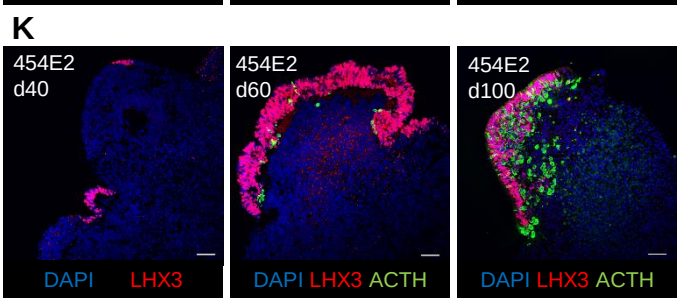
K
454E2 d40
454E2 d60
454E2 d100
DAPI LHX3
DAPI LHX3 ACTH

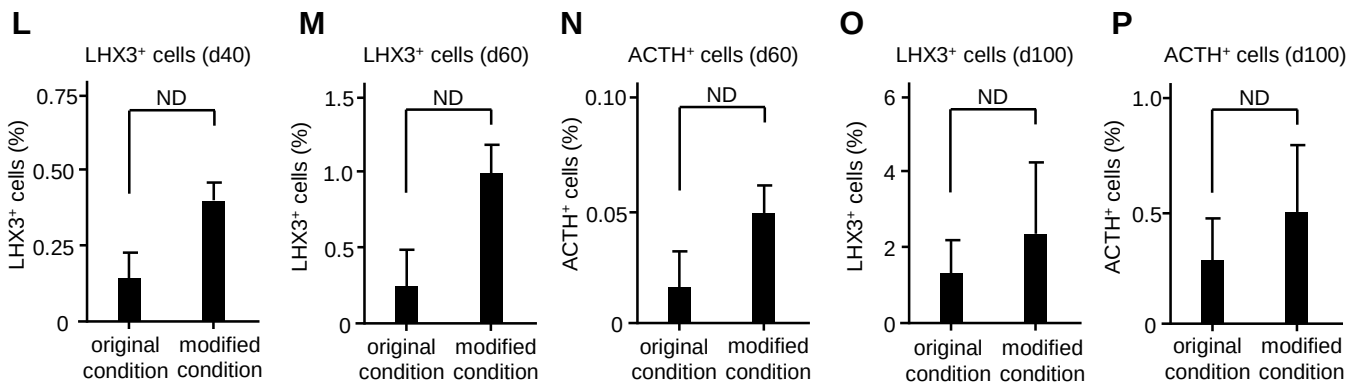
L
LHX3+ cells (d40)
M
LHX3+ cells (d60)
N
ACTH+ cells (d60)
O
LHX3+ cells (d100)
P
ACTH+ cells (d100)
ND
LHX3+ cells (%)
ACTH+ cells (%)
original condition
modified condition

Figure S3. Induction of human iPS cell line 409B2 and 454E2 to differentiate into anterior pituitary. Related to Figure 1.

(A–H) Data of human iPS cell line 409B2.
(A) Induction of differentiation of 409B2 cells under the original condition. $LHX3^+$ cells and $ACTH^+$ cells were observed in oral ectoderm-like tissue.
(B) Modified condition for 409B2 cells. The BMP4 concentration was changed to 10 nM.
(C) LHX3 and ACTH immunostaining.
(D–H) Proportion of $LHX3^+$ cells and $ACTH^+$ cells, as determined by immunostaining (n = 5 experiments). $LHX3^+$ cells and $ACTH^+$ cells tended to be abundant under the modified condition but without statistical significance.

(I–P) Data of human iPS cell line 454E2.
(I) Induction of differentiation of 454E2 cells under the original condition. $LHX3^+$ cells and $ACTH^+$ cells were observed in oral ectoderm-like tissue.
(J) Modified condition for 454E2 cells. The KSR concentration was changed to 10 nM, and the number of cells per well was changed to 10,000.
(K) LHX3 and ACTH immunostaining.
(L–P) Proportion of $LHX3^+$ cells and $ACTH^+$ cells, as determined by immunostaining (n = 3 experiments). $LHX3^+$ cells and $ACTH^+$ cells tended to be abundant under the modified condition, but without statistical significance.

Values shown on graphs represent means ± s.e.m. *$P<0.05$.
Scale bars: 50 μm (A, C, I, K).

Figure S4

A

Batch number	Number of aggregates containing both ACTH$^+$ cells and CRH$^+$ cells	Total number of aggregates
1	2	6
2	2	9
3	1	8
4	0	8
5	1	9
6	1	8
7	1	8
8	1	8
total	9	64

B

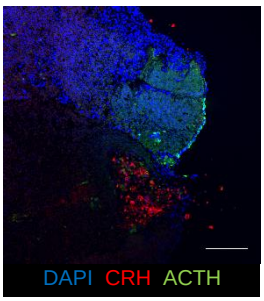

C

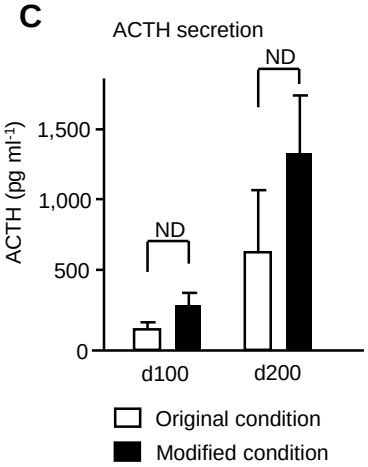

D

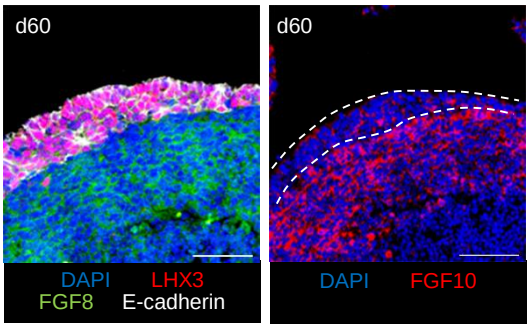

E

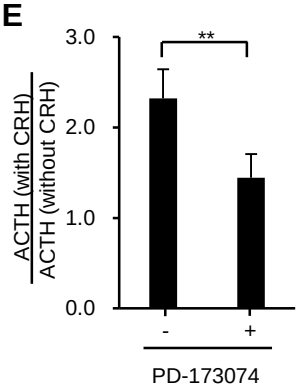

Figure S4. Additional data of hybrid aggregates. Related to Figures 2 and 3.

(A) Number of aggregates containing both $ACTH^+$ cells and CRH^+ cells on day 200 in each batch.
201B7 cells were cultured under the modified condition. Aggregates were evaluated on day 200.

(B, C) Hybrid aggregates are also induced in long term culture under the original condition.
(B) Hybrid aggregates were also induced under the original condition.
(C) ACTH levels in the culture supernatant tended to be higher under the modified condition [modified condition, n = 22 (day 100), 11 (day 200) experiments, original condition, n = 17 (day 100 and 200) experiments].

(D, E) FGF signals as hypothalamic factors.
(D) Expression of FGF8 and FGF10 in the inner layer of hybrid aggregates.
(E) ACTH secretion ability on day 120 was suppressed by treatment with an FGF receptor inhibitor. PD-173074 was added at 10 nM (n = 4 experiments).

Values shown in graphs represent means ± s.e.m. *P<0.05; **P<0.01; ***P<0.001.
Scale bars: 200 μm (B), 50 μm (D).